Ocean and Coastal Management 246 (2023) 106903

Contents lists available at ScienceDirect

Ocean and Coastal Management

journal homepage: www.elsevier.com/locate/ocecoaman

The hyperturbid mesotidal Guadalquivir estuary during an extreme turbidity event: Identifying potential management strategies

César Megina [a,*], Íñigo Donázar-Aramedía [b], Juan Miguel Miró [b], Jesús García-Lafuente [c], José Carlos García-Gómez [b]

[a] Biodiversidad y Ecología Acuática, Departamento de Zoología, Facultad de Biología, Universidad de Sevilla, Sevilla, Spain
[b] Laboratorio Biología Marina, Área de Investigación Biológica I + D + I del Acuario de Sevilla, Departamento de Zoología, Facultad de Biología, Universidad de Sevilla, Sevilla, Spain
[c] Grupo Oceanografía Física, Instituto de Biotecnología y Desarrollo Azul (IBYDA), Universidad de Málaga, Málaga, Spain

ARTICLE INFO

Keywords:
Guadalquivir estuary
Turbidity
Suspended particulate matter
Persistent hyperturbid events
Light limitation
Hypoxia

ABSTRACT

The Guadalquivir estuary (SW Iberian Peninsula) is a mesotidal system within a Mediterranean climatic region. It experiences severe and persistent hyperturbid conditions during the wet and cold season, significantly impacting both the ecosystem and various economic activities.

During an investigation of an extreme turbidity event, suspended particulate matter (SPM) concentrations exceeding 30 g/L were found near the salt intrusion limit, with a 45 km stretch showing a depth-averaged SPM concentration greater than 10 g/L. Throughout this event, the estuary can accumulate more than 900,000 tonnes of SPM, leading to severe surface light blockage, with the euphotic layer remaining shallower than 10 cm in most areas. Additionally, hypoxia develops in the zone of maximum turbidity, near the bottom.

These extreme turbidity events are linked to short-duration freshets that discharge a large amount of sediment from a highly erodible catchment area, followed by a significant reduction in river flow, primarily due to strong water regulation. However, hyperturbid conditions never extend into the summer in this estuary, indicating a non-negligible capacity to clear the SPM.

Considering these findings, several recommendations are proposed. First, establishing a monitoring programme for extreme turbidity processes can aid in implementing necessary management actions. Second, it is crucial to develop an optimal protocol for water discharges from the network of dams to maximise sediment export to the sea, minimise plankton washout, and prevent excessive freshwater loss.

1. Introduction

Human activities have significantly impacted the hydrological patterns of rivers, resulting in profound changes in sediment dynamics within estuaries. Various anthropogenic pressures, including land clearance, overgrazing, and agricultural practices, have led to soil erosion in river watersheds. Consequently, increased levels of suspended particulate matter (SPM) and turbidity have been observed (Wolanski, 2004). Conversely, the construction of dams for flood control, water storage, and power generation has the potential to reduce sediment discharge into estuaries by trapping these sediments (Vörösmarty et al., 2003). However, it is important to note that dam trapping primarily affects coarse sediments, and even in regulated watersheds, fine sediment can still find its way into estuaries, altering the composition of estuarine and coastal substrates from sand to mud and increasing turbidity (Wolanski, 2004). Moreover, the transport of fine sediment to the sea is closely associated with river forcing (Jay et al., 2007; Burchard et al., 2018), and the reduction in river flow caused by damming and water diversion hampers the effective flushing of SPM, which becomes more susceptible to entrapment within estuaries (Wolanski, 2004; Uncles et al., 2013; Jalón-Rojas et al., 2015).

Several regulated European estuaries have been found to accumulate substantial amounts of SPM, leading to the development of hyperturbid conditions, often exceeding several grammes per litre. In particular, SPM accumulates in zones known as estuarine turbidity maxima (ETM). This can be observed in estuaries such as the Charente (Toublanc et al., 2016), the Gironde (Jalón-Rojas et al., 2015), the Humber (Uncles et al., 2006), the Seine (Grasso et al., 2018), among others. Elevated turbidity

* Corresponding author. Departamento de Zoología, Facultad de Biología, Universidad de Sevilla, Av. Reina Mercedes 6, 41012, Sevilla, Spain.
E-mail address: cmegina@us.es (C. Megina).

https://doi.org/10.1016/j.ocecoaman.2023.106903
Received 27 April 2023; Received in revised form 19 October 2023; Accepted 21 October 2023
Available online 25 October 2023

levels in estuaries give rise to various environmental issues. For instance, the reduced light penetration in the water column limits primary production and causes a shift in estuarine metabolism towards a more heterotrophic state (Ruiz et al., 2017). Additionally, high turbidity adversely affects water quality by decreasing oxygen concentration, primarily due to reduced photosynthetic activity and increased oxygen demand resulting from organic matter degradation (Schmidt et al., 2019). Furthermore, the presence of high turbidity can have several impacts on biota, including alterations in predator-prey interactions and food webs, reduced food availability, compromised visibility, and negative health effects (Bruton, 1985; Hecht and van der Lingen, 1992; Utne-Palm, 2002; Bilotta and Brazier, 2008; González-Ortegón et al., 2010).

The accumulation of fine sediment and SPM within estuaries, as well as the formation of ETM, can be driven by various hydrodynamic processes (Burchard et al., 2018). Density-driven estuarine circulation is one of the primary mechanisms, responsible for directing the residual current along the bottom, where the SPM concentration is higher, up the estuary. Additionally, tidal pumping, associated with flood-dominant conditions, leads to increased resuspension and transport of SPM during floods, also contributing to the up-estuary movement (Uncles et al., 2002; Mitchell, 2013; Burchard et al., 2018). These mechanisms are influenced by the intrinsic characteristics of the estuaries. Uncles et al. (2002) demonstrated that the concentration of SPM is influenced by factors such as tidal range and the length of tidal intrusion. Estuaries with longer lengths and greater tidal influence tend to exhibit longer residence times of water and solutes, higher resuspension capacity of fine sediments, and stronger tidal pumping capabilities. Human modifications of estuaries, including canalisation, deepening, and extensive removal of intertidal areas, can also impact these mechanisms, resulting in upstream tidal amplification and increased transport of SPM upstream (Mitchell and Uncles, 2013; Winterwerp et al., 2013; Wang et al., 2014).

These processes interact with other intrinsic characteristics of the watershed, including its size, topography, rainfall regime, geology, morphology, and erosivity. This interaction results in a distinct equilibrium between sediment provision and removal of SPM that is specific to each estuary (Uncles et al., 2002; Milliman and Farnsworth, 2011).

Most of the available information on sediment dynamics in European hyperturbid estuaries is primarily related to macrotidal systems or those in the transition between mesotidal and macrotidal environments, predominantly located in the cold temperate region (Uncles et al., 2006; Jalón-Rojas et al., 2015; Toublanc et al., 2016; Grasso et al., 2018). In this region, a distinct wet season is typically observed, characterised by sustained high river flow, which facilitates the export of SPM to the sea (Piton et al., 2020). Consequently, these estuaries often exhibit their highest levels of turbidity during the low river flow season when the sediment export capacity to the sea is reduced, causing the zone of fine sediment accumulation (ETM) to shift upstream (Uncles et al., 2002; Mitchell, 2013; Jalón-Rojas et al., 2017).

The Guadalquivir estuary, located in the southwest of the Iberian Peninsula (Fig. 1), is a mesotidal system in a warm-temperate region characterised by a Mediterranean regime with Atlantic influence. This region experiences dry, hot, and extended summers, with rainfall below 10 mm and maximum temperatures that can exceed 40 °C. Mild, wet winters and irregular, often torrential rainfall (annual average 630 mm) are also typical (Sabater et al., 2009). Information on sediment dynamics in such estuaries is relatively limited. Empirical observations and theoretical predictions suggest that mesotidal estuaries tend to have lower intrinsic levels of suspended particulate matter (SPM) compared to macrotidal and hypertidal estuaries (Uncles et al., 2002; Schoellhamer, 2011). However, the Guadalquivir estuary is a hyperturbid system that has garnered international attention due to the recurrent formation of large turbidity plumes during flood events (evidenced, for example, at https://earthobservatory.nasa.gov/images/79677/sediment-plume-along-the-coast-of-spain). In fact, it has the largest and most turbid plume among the major rivers in the Iberian Peninsula, despite having the second smallest discharge (Fernández-Nóvoa et al., 2017). This estuary consistently exhibits high concentrations of SPM and regularly experiences extreme and persistent turbidity events (González-Ortegón et al., 2010), to the extent that it has been referred to as the second most turbid estuary in the world, after the Ganges (Ruiz et al., 2015, 2017). Such high turbidity and suspended sediment concentrations not only impact biological communities, as previously explained (González-Ortegón et al., 2010; Donázar-Aramendía et al., 2018; Miró et al., 2022), but also pose significant challenges for activities such as aquaculture (as reported at https://www.elmundo.es/andalucia/2021/12/02/61a91328fdddffdc528b4575.html).

The Guadalquivir River basin has undergone significant

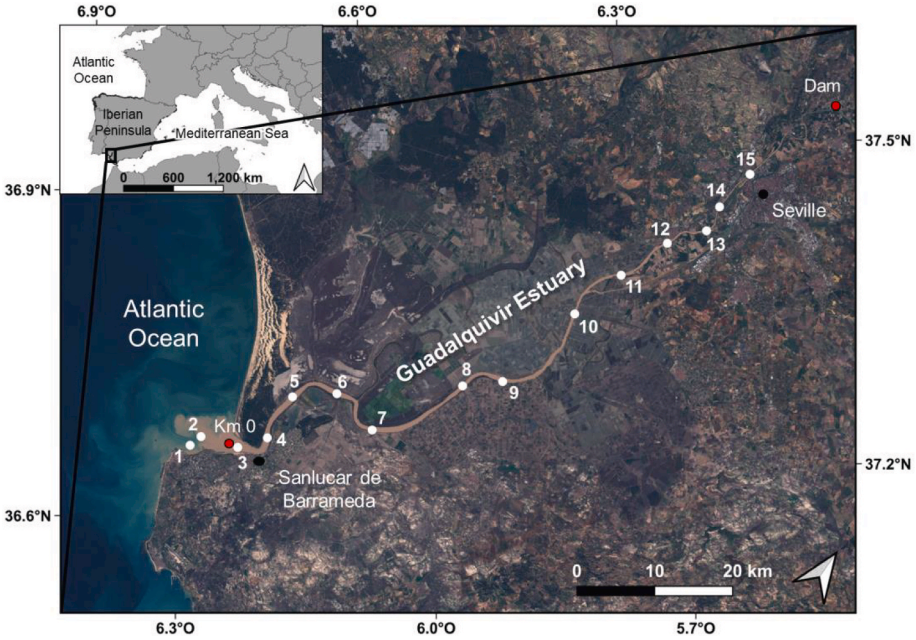

Fig. 1. Study area. Numbers 1–15: sampling points for vertical profiles of physical-chemical variables and water samples. Km 0: the initial point of the estuary. Dam: Alcala del Río dam, the upstream limit of the estuary.

transformation and alteration, including intense damming (118 dams; García-Martínez and Rinaldi, 2022) and extensive water abstraction, mainly for agricultural purposes. These activities have resulted in a reduction of river discharges by over 50% (González-Ortegón et al., 2010). The hydrological regime exhibits strong seasonality and marked extremes, and the basin has a high percentage of its surface dedicated to agriculture (Sabater et al., 2009). Consequently, the Guadalquivir River watershed has a high sediment yield, estimated to exceed 282 t km^{-2} y^{-1} on average, with maximum values reaching up to 1415 t km^{-2} y^{-1} (Buendia et al., 2016). Since 1795, the main channel of the Guadalquivir River has experienced multiple artificial meander cut-offs to facilitate navigation to Seville (Baena-Escudero et al., 2019). Furthermore, over 70% of the adjacent marshlands have been transformed into cultivated fields for various purposes, including agriculture, aquaculture, and saltponds (Zorrilla-Miras et al., 2014; Ruiz et al., 2015). These alterations have resulted in a significant reduction of the original intertidal area and, consequently, tidal flooding (Ruiz et al., 2015; Llope, 2017). The Guadalquivir estuary provides access to the only inland port on the Iberian Peninsula, the port of Seville, which requires regular dredging to maintain the depth of the navigation channel (Donázar-Aramendía et al., 2018; Miró et al., 2022). Despite these challenges, the Guadalquivir estuary paradoxically serves as the main nursery ground, exhibiting higher productivity and a more complex and interconnected food web compared to other estuaries in the region (Donázar-Aramendía et al., 2019; Miró et al., 2020).

This estuary serves as a convergence point for various social and economic interests, often conflicting with each other. These include nature conservation (including Doñana National Park, a World Heritage Site), commercial maritime traffic, rice and other crop farming, freshwater management, hydroelectric energy, coastal and eco-tourism, and aquaculture (Ruiz et al., 2015). The issue of excessive turbidity is a matter of concern in this context, which requires reliable observations of SPM and related parameters such as dissolved oxygen to gain a better understanding of their dynamics. This knowledge is crucial for developing management strategies that promote sustainable activities and improve estuary health (Schmidt et al., 2019).

However, the available information on turbidity, SPM, and other variables remains partial. Most data come from near-surface measurements, either from fixed sensors (Navarro et al., 2011; Díez-Minguito et al., 2014) or satellite observations (Carpintero et al., 2013; Caballero et al., 2014; Caballero and Navarro, 2016). Comprehensive depth-integrated information on these variables is still lacking. Additionally, the question of whether turbidity is primarily controlled by sediment supply or tidal forces is still a topic of discussion (González-Ortegón et al., 2010; Díez-Minguito et al., 2014; Ruiz et al., 2017). Addressing this essential question is crucial when considering potential management approaches for these processes.

During winter 2019–2020, the Guadalquivir estuary experienced an extreme turbidity event. This article aims to provide a comprehensive analysis of the spatial physicochemical characteristics throughout the water column during this event, including SPM, oxygen, light penetration, and salinity. The study covers a wide range, from several kilometres nearshore to the estuary to its head, allowing for a detailed understanding of the conditions during this period. Furthermore, the paper also reviews existing information, discusses the origins and dynamics of these turbidity processes, and identifies potential areas of interest for future research. Further, the study explores possible management approaches to address this environmental issue.

2. Material and methods

To document this extreme turbidity event, vertical profiles of the main physicochemical variables were obtained on 2020-01-21, at 15 stations along the main channel (Fig. 1). The first profile was taken immediately outside the river plume visually identified from the boat, the second profile was collected inside the river plume, and the following 13 profiles were performed at intervals, closer where more intense changes were expected (based on our previous experience), up to 87 km from the river mouth (Fig. 1). In this study, we report data on salinity, SPM, oxygen saturation, and photosynthetically active radiation (PAR), supplemented with relevant data on temperature and oxygen concentration. To provide more standardised information and taking advantage of the tidal propagation period into the estuary, all stations were surveyed during flooding at approximately local high water (HW), following the criteria used by Uncles et al. (2006). To estimate the sampling time with respect to the tide, we used water level data from two tide gauges (https://www.puertos.es/en-us/oceanografia/Pages/portus.aspx), one installed at the entrance of the estuary (Sanlucar de Barrameda, Fig. 1) and one approximately 80 km upstream, at the entrance of the Seville port (Seville, Fig. 1).

Water samples were collected at all stations using a Van Dorn bottle, both in midwater and, in some stations, near the bed (bottom depth ranging from 6.3 to 11.2 m), to determine the SPM and establish a relationship between turbidity and SPM. Salinity, temperature, oxygen concentration, and saturation, as well as turbidity up to 3500 NTU (Nephelometric Turbidity Units), were measured *in situ*, from the boat, using a multiprobe (Eureka Manta 2; Eureka Water Probes, Austin, USA). This probe measures light scattered at an angle of 90° and has a range of 0–4000 NTU. Turbidity values higher than this limit were measured with a back-scatter turbidity probe (Analite NEP-5000 Turbidity Meter; Observator Instruments, Ridderkerk, Netherlands) with a range of 0–30,000 NTU. Turbidity values lower than 3500 NTU were measured more precisely with the first probe.

Water samples were filtered through precombusted (4 h, 500 °C) filters with a pore size of 0.7 μm (Whatman GF/F). The filters were then dried (24 h, 60 °C) and weighed to obtain the SPM concentration. Linear regression was used to fit the SPM concentration with the corresponding turbidity measures for values below 3500 NTU ($p < 0.0001$, $R2 = 0.9732$; Supplementary Fig. 1A). For higher turbidity values, a second-order polynomial regression was fitted using the backscatter sensor data and the corresponding SPM measures ($p < 0.0001$, $R2 = 0.9871$; Supplementary Fig. 1B). Vertical profiles of SPM for each station were obtained from NTU profiles using these models. Smoothing functions were fitted to the SPM and other variable profiles using an additive model with the mgcv package (v1.8-40, Wood, 2017) in R statistical software (R Core Team, 2022). Predictions from these models were represented in 2D figures using Ocean Data View (Schlitzer, 2021) and were also used to obtain depth-averaged values. Additionally, the average of modelled SPM in the top metre of the water column was used to replicate the results that could have been obtained from satellite or near-surface sensors, which could then be compared with published data for the Guadalquivir estuary.

The water volume of the Guadalquivir estuary upstream of km 0 (Fig. 1) is used to assess the total mass of SPM in the whole estuary. It has been computed from the bathymetric data collected by the Port Authority of Seville in years 2019 and 2021 for the non-navigable and navigable part of the estuary, respectively. The data was projected onto a rectangular grid along the river that covered the entire estuary. The number of grid cells is over 15,000, with a mean size of 97 × 44 m and an assigned depth given by the average of all data points within the cell. Since bathymetry refers to the mean sea level, this volume corresponds to the tidally averaged estuary.

Scalar PAR irradiance at different depths [$E_0(z)$] was measured as photon flux density (μmol s^{-1} m^{-2}) using an underwater spherical sensor (LI-COR® LI-193). To account for variations in ambient light, the downwelling irradiance, measured in air with a 180° sensor (LI-COR® LI-190R), was used as a reference [$E_d(ref)$] (Pilgrim, 1987). To account for short-term variability in light intensity arriving at the sensor (Kirk, 1994), each measurement was integrated over 15 s. When it was possible to obtain multiple measurements at different depths (see the section 'Results'), the depth-mean PAR extinction coefficient (K_0) was calculated from the slope of the $-\ln[E_0(z)/E_d(ref)]$ profiles (Pilgrim 1987).

To provide a more comprehensive understanding of this extreme turbidity process, average daily rain (from 49 pluviometers throughout the catchment area), river discharge, and surface level data at the estuary head were obtained from the Automatic Hydrological Information System (Confederación Hidrográfica del Guadalquivir: https://www.chguadalquivir.es/saih/), and hourly significant wave height in the Gulf of Cádiz (6.96° W, 36.49° N) and water level at the mouth of the estuary from Puertos del Estado (https://portus.puertos.es/).

3. Results

During a short period of 16–21 December 2019, the catchment area experienced intense rain, particularly heavy during the three days between 19 and 21 December. This resulted in a discharge of 1105 m^3/s (daily mean) on 22 December 2019 (Fig. 2A), and a notable increase in the water level in the estuary head during this time (Fig. 2B).

On the ocean side of the estuary, meteorological conditions led to higher significant wave heights in the Gulf of Cadiz (Fig. 2B) and a meteorological tide that elevated the sea level at the mouth of the estuary (Fig. 2A). Subsequently, there was a sharp reduction in dam discharge, which remained below 40 m^3/s a few days after the flood and even below 30 m^3/s during the initial days of 2020 at the start of the subsequent neap tide (Fig. 2A).

On the day of sampling (21 January 2020), it was a neap tide with an average tidal range (± standard deviation) of 1.58 ± 0.07 m (Fig. 2A), measured by a tide gauge at the mouth of the estuary.

Fig. 3 shows the evolution of the river plume during this period.

3.1. Turbidity, SPM, and salinity

The result was an event of extreme turbidity, with SPM concentrations greater than 30 g/L (maximum measured concentration = 30,940 mg/L; maximum estimated concentration = 31,217 mg/L) in the near-bed layer 70–75 km upstream of the river mouth (profile 12, Fig. 4A). The zone with maximum SPM concentration was located near the isohaline of 1 psu (Fig. 5A). Fig. 5A shows the salinity in the estuary 29 days after the freshet, which shows the vertically well-mixed structure.

If we define an ETM based on the depth-averaged SPM concentration (daETM), it can be identified as a 45 km long stretch with a depth-averaged SPM concentration greater than 10,000 mg/L, extending from approximately km 25 (profile 7) to km 70 (profile 12) (Fig. 4B). The downstream limit of daETM (profile 8) had the maximum depth-averaged SPM concentration of 12,447 mg/L, and the stratification of SPM in the water column intensified progressively upstream, leading to higher concentrations near the bed and lower concentrations near the surface upstream of daETM (Fig. 4A).

Furthermore, based on the maximum near-bed SPM concentration, a core ETM can be defined as a longitudinal region of approximately 35 km, where the SPM concentration near the bed exceeds 20,000 mg/L, approximately between km 50 and km 85 (Fig. 4A). The landward limit of this core ETM exhibits near-bed SPM concentrations exceeding 30,000 mg/L, primarily located upstream of the daETM (profiles 12, 13, and 14; Fig. 4A and B). Moreover, a separate secondary maximum can be observed around 65 km (profile 10) with slightly higher stratification and a near-bed SPM concentration exceeding 25,000 mg/L.

The predictions of the additive model graphically represented in Fig. 4B allow us to calculate an average single value of SPM concentration for the entire studied section of 3145 mg/L (depth-averaged and from km 0 to the upper sampling point, approximately km 87; Fig. 1). Using the bathymetry data provided by the Port Authority of Seville, we can approximate the total volume of the estuary to be close to 290 hm^3. Based on the estimated average SPM concentration for the entire estuary, the total mass of SPM during the sampling time would exceed 900,000 tonnes.

When focussing only on the data from the first metre (Fig. 4C), the maximum concentration of SPM would be 5461 mg/L, observed 25–30 km from the river mouth. Moving upstream from this point, the SPM concentration would progressively decrease, together with an intensification of stratification in the water column (Fig. 4C).

3.2. Light availability and oxygen

On the sampling day, the weather was clear with only a few clouds, resulting in downwelling irradiances (PPFD) at the water surface ranging mainly between 1700–1200 μmol s^{-1} m^{-2}, occasionally dropping to 700-500 μmol s^{-1} m^{-2}. Under these conditions, light penetration was limited and it was only detectable below −1 m in the first profile outside the river plume. At 4 m depth in this profile, the irradiance measured 0.05 μmol s^{-1} m^{-2} and fell to 0 at deeper levels (Supplementary Table 1). The calculated extinction coefficient K_0 at this point was 2.28 m^{-1}, reaching the euphotic zone at −2 m (Z_{eu}). Within the river plume, in the first profile (profile 2), light was detectable up to −1 m. The estimated K_0 was 10.58 m^{-1}, and Z_{eu} extended to about 40 cm deep. Moving upstream, light penetration gradually decreased and in profile 5

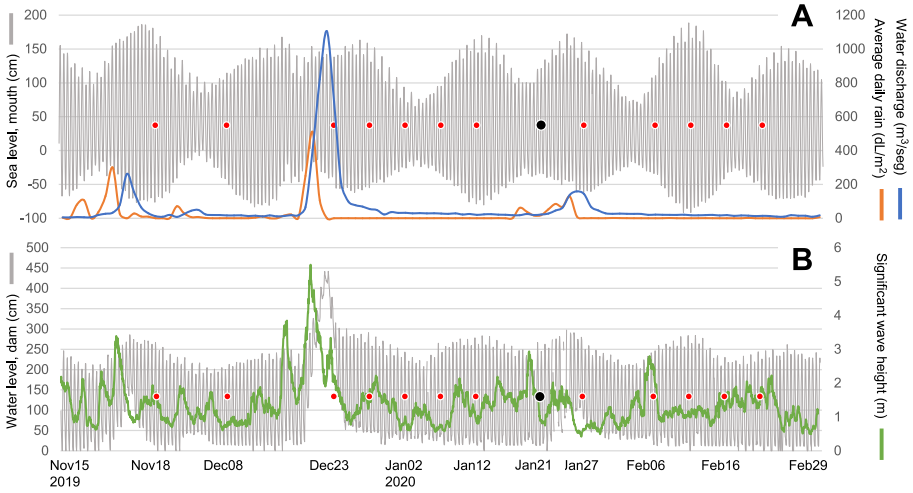

Fig. 2. Temporal evolution of some environmental variables during the studied hyperturbid event in the Guadalquivir estuary. A: sea level in the entrance of the estuary (grey line), average daily rain in the catchment area (orange line), water discharge from the Alcalá del Río Dam (blue line); and B: water level just below the last dam (grey line), significant wave height in the Gulf of Cádiz (green line). Black point: Day of sampling. Red points: Days of satellite images from Fig. 3.

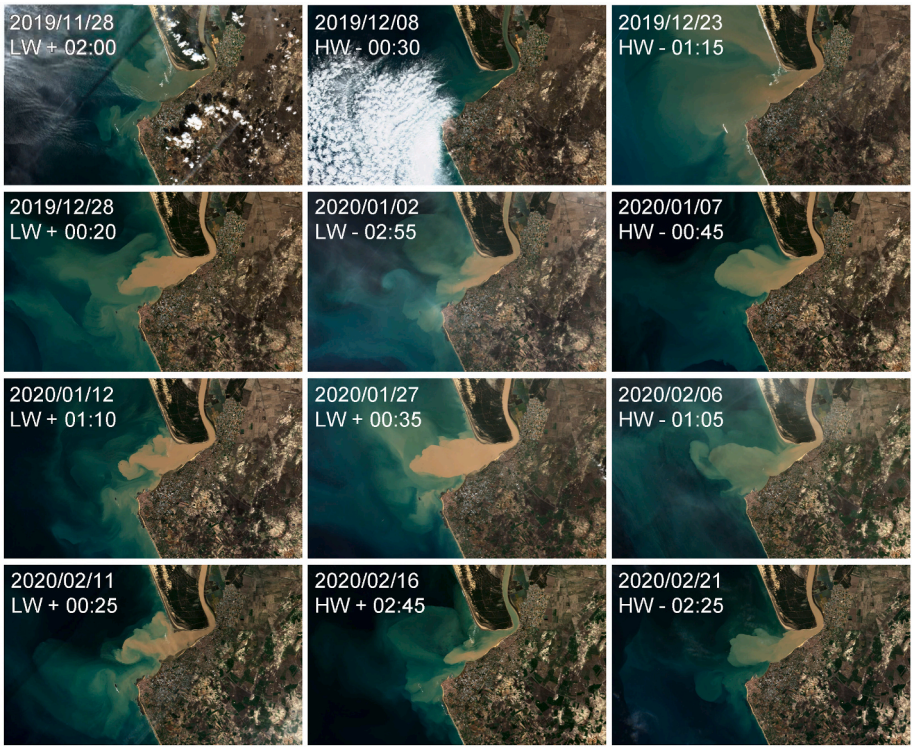

Fig. 3. Satellite images of the Guadalquivir estuary mouth in the studied period. Satellite images were all collected with Sentinel-2 at 11:21 UTC. Each image is referenced to the date of collection and the nearest high or low water (HW/LW) plus or minus the time in hours and minutes to 11:21 UTC.

(approximately 13.5 km from the river mouth), scalar irradiance, from all directions, at the first depth of measure (approximately 10 cm deep) was 0.01 μmol s^{-1} m^{-2}. As we proceed further upstream, light remained completely blocked at the surface until the last profile. Irradiances between 0.00 and 0.02 μmol s^{-1} m^{-2} were observed up to profile 9 (approximately 44.5 km), and from profile 10–15, it increased to around 1 μmol s^{-1} m^{-2} (Supplementary Table 1).

In connection with this, hypoxia was observed near the bed in the core ETM and upstream from this point (Fig. 5B: oxygen saturation isolines of 20%, 30%, and 40% correspond approximately to oxygen concentrations of 2, 3, and 4 mg/L). Oxygen values below 3 mg/L and saturations below 30% were measured in the last metre of profiles 12, 13, and 14. Approximately 75 km from the river mouth, in profile 12, a minimum oxygen concentration of 1.3 mg/L and a saturation of 12% were detected at the bottom.

4. Discussion

4.1. Turbidity and estuarine turbidity maximum

Associated with stormy weather in the region, the observed event of extreme turbidity was the result of a short-lived peak of freshwater discharges from the watershed, followed by a sharp reduction in the discharge a few days after the flood. In fact, the vertically well-mixed structure of the estuary with respect to salinity, observed one month after the freshet, is typical of tidally dominated estuaries as a consequence of strongly regulated flow (Ruiz et al., 2015).

Like in many estuaries, the zone with the highest concentration of SPM near the bed, which we defined as the core ETM, was found near the limit of salinity intrusion (Burchard et al., 2018). In our study, the pattern of SPM distribution in the Guadalquivir estuary was similar to that described by Uncles et al. (2006) for the macrotidal Humber estuary in the UK. In this work, the ETM was defined as a 35 km longitudinal region where the concentration of SPM near the bed exceeds 16 g/L, with a considerable portion within this ETM where the SPM concentrations exceed twice this value (>32 g/L), reaching maximum values of 47 and 45 g/L during spring and neap tide, respectively. The head of this ETM was also situated near the isohaline of 1 psμ.

In addition, we also defined an ETM based on the depth-averaged SPM concentration, which gives a better representation of the total sediment pool in a specific section of the estuary at a given time. The location of the core ETM, predominantly outside the daETM, indicates a lower total amount of sediment in the water column of this stretch, with a significant amount of this sediment concentrated in the deepest layers. This, together with the observed progressive intensification of SPM stratification within the daETM as we move upstream, indicates sediment settle in this section of the estuary. And, in fact, this zone is adjacent to the entrance to the port of Seville, where the Port Authority must dredge to maintain navigation depth with greater frequency and intensity (Díez-Minguito et al., 2012), as an indication of effective deposition of SPM on the bed.

In previous studies of the Guadalquivir estuary, a primary ETM was also identified near the limit of salinity intrusion approximately 80 km from the river mouth, characterised by a maximum SPM concentration of around 1 g/L (Díez-Minguito et al., 2014). This was also at a neap tide as in the present study, but during a period of low river discharge. This classical ETM appears to occur under various circumstances in this estuary. The position of the ETM can offer information on the dominant mechanisms responsible for its formation, and an ETM located at the landward limit of salt intrusion is often associated with estuarine circulation (Mitchell, 2013; Burchard et al., 2018). However, Díez-Minguito et al. (2014) noted that vertically sheared mean flows would represent a smaller contribution to the generation of turbidity maxima, while tidal pumping could play a more significant role. Understanding the dominant mechanisms behind the formation of ETM is crucial for the development of effective management strategies to address excessive turbidity. For example, in cases where tidal pumping is the main mechanism, stronger currents during spring tides could promote landward transport of SPM, while sediment export to the sea could potentially be increased during neap tides. Conversely, if estuarine circulation

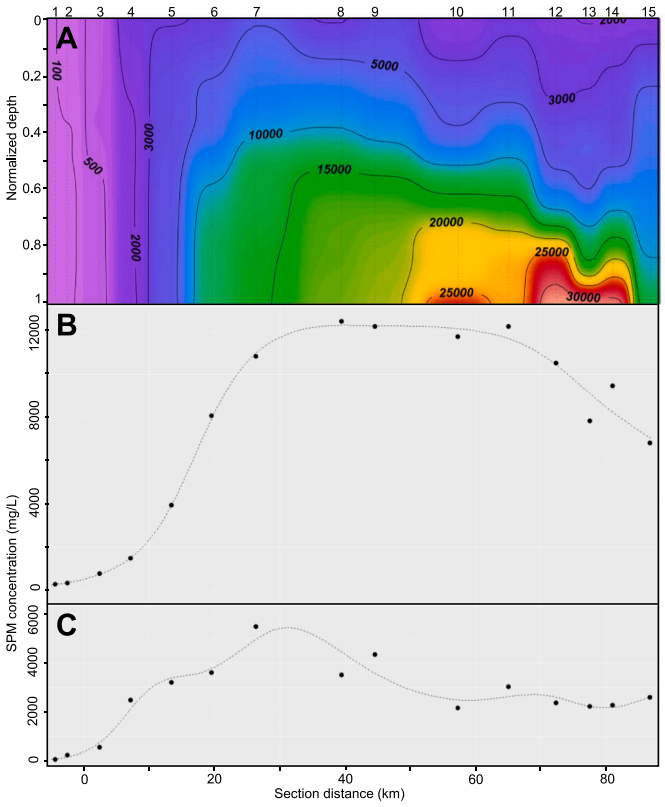

Fig. 4. The x axis is section distance, common for all 3 graphs. A) 2D profile of SPM concentration (isolines in mg/L). Sampling points where vertical profiles were performed are marked as vertical dotted lines. B) Depth averaged SPM concentration at every sampling point. Dashed line is a smoothing line representing the prediction of an additive model relating section distance and depth averaged SPM concentration. C) The same as B but using only data from the first metre.

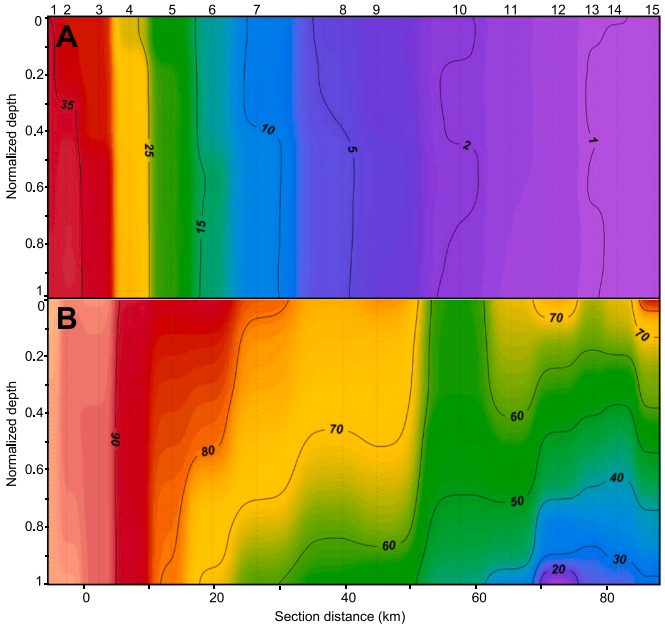

Fig. 5. 2D profile of A) salinity (isolines in practical salinity units) and B) oxygen saturation (isolines in %). Sampling points where vertical profiles were performed are marked as vertical dotted lines. The x axis is section distance, common for the 2 graphs.

prevails, the opposite trend could be observed (Burchard et al., 2018). In this regard, Contreras (2012) recommended maintaining a higher water flow during neaps to promote sediment export, instead of a homogeneous low flow, in agreement with the results of Díez-Minguito et al. (2014).

These latter authors also identified two additional secondary ETMs at 35 and 58 km (a few km downstream of our profiles 8 and 10 respectively) with concentrations of up to 0.86 and 0.99 g/L, respectively. Other previous studies based on satellite remote sensing had also identified an ETM between 20 and 30 km from the estuary mouth (SPM concentration of 0.40–0.55 g/L), with this concentration decreasing when moving up the estuary (Caballero et al., 2014). The presence of multiple ETMs is common in estuaries, under the variable influence of tidal and fluvial forcing, estuarine circulation, topography, and aided by various mechanisms of flocculation (Jay et al., 2007; Burchard et al., 2018; Vinh and Ouillon, 2021). In the Guadalquivir estuary, the formation of these secondary ETMs has been associated with the effect of the tidal wave reflecting on the dam and propagating in the opposite direction to the incoming tide. This generates convergence zones between sections of net seaward SPM transport and sections of net landward transport (Díez-Minguito et al., 2012, 2014). Furthermore, the lower secondary ETM is located near marked meanders with relatively low curvature radius, which enhances secondary flow and contributes to maintaining high turbidity levels (Ruiz et al., 2015). However, during the period of extreme turbidity studied here, the presence of these secondary ETMs has not been clearly identified, probably due to the substantial amount of SPM accumulated in the estuary. However, the observation of a secondary maximum near the bed in profile 10 could still indicate the influence of the hydrological processes documented by Díez-Minguito et al. (2014).

Identification of the actual structure of the water column in relation to SPM and its concentration values can be challenging when relying solely on data collected near the surface, either sensors near the surface or satellite imagery. In our analysis of the SPM data within the first metre of the water column, we observed a scenario similar to that described by satellite imagery (Caballero et al., 2014). In this view, the secondary ETM near 20–30 km that these authors described is also visible, as well as the continuous decrease in SPM concentration upstream this point. Uncles et al. (2006) documented that apparent maximum values of SPM concentration on the surface occur during periods of maximum current speed and bed shear, leading to maximum SPM resuspension and water column homogenisation. However, the actual maximum values are more likely to occur in opposite conditions, near the bed during high water slack, when maximum column stratification is present (Uncles et al., 2006; Mitchell, 2013). Comprehensive studies of the Guadalquivir estuary, which relied on a network of sensors collecting continuous data from the near surface over three years, including periods of extreme turbidity, reported maximum SPM values of 5388 mg/L (Ruiz et al., 2017). These values are comparable to those observed in our study when considering data from the first metre (5461 mg/L). However, near-bed measurements showed concentrations that exceeded 5–6 times this value. Variability in near-surface SPM concentration, both temporally and spatially, may be attributed to changes in the degree of stratification, making it challenging to distinguish from real changes in total SPM concentration due to effective deposition. While continuous monitoring using fixed sensors and easy access to data through remote satellite imagery are undeniably valuable, it would be advisable to complement these views with a more depth-integrative approach to obtain a more accurate representation of the characteristics of the water column.

Regarding the claim that the Guadalquivir estuary is the second most turbid in the world after the Ganges, even with the increased maximum SPM concentration observed in this study, other publications have reported higher SPM concentrations in various estuaries [see, for instance, Uncles et al. (2002) and references therein]. While its exact position in the ranking of turbid estuaries may vary, the Guadalquivir estuary

possesses an important distinctive characteristic: it is a mesotidal system. On the contrary, most other estuaries with higher or similar turbidity are macrotidal and, consequently, have a higher capacity of tidal resuspension and maintenance of SPM. This observation suggests that the focus for environmental improvement should perhaps shift toward addressing the input of sediment from the highly erodible catchment area, rather than mainly on tidal resuspension, as previously suggested (Díez-Minguito et al., 2014; Ruiz et al., 2015, 2017).

4.2. The genesis of high turbidity periods

In other rainier regions, periods of higher turbidity have often been associated with quiescent weather conditions and low sustained river discharges. This trend has been observed in temperate European macrotidal estuaries such as the Humber in the UK (Uncles et al., 2006), the Gironde in France (Jalón-Rojas et al., 2015), the Loire in France (Jalón-Rojas et al., 2016), and the Charente in France (Modéran et al., 2010). Similar patterns have also been documented in the monsoonal tropical mesotidal Cam Nam Trieu (Vinh and Ouillon, 2021) and the macrotidal Van Uc in Vietnam (Piton et al., 2020). During the wet season, with sustained high river flow, the ETM is typically advected downstream, leading to higher export of SPM (Piton et al., 2020). In contrast, when river flow decreases and sediment input diminishes, tidal resuspension and entrainment contribute to increased turbidity. In the short term, the variability in SPM concentration is associated with tides, with maximum levels occurring during spring tides when the tidal strength is at its peak (Uncles et al., 2006; Jalón-Rojas et al., 2016; Burchard et al., 2018). However, these maximum levels can be influenced, to some extent, by the fluvial supply. For example, in an analysis of interannual variability in the Gironde and Loire, Jalón-Rojas et al. (2015, 2016) found that the concentration of SPM in the ETM during the dry period correlated well with the freshwater volume previously discharged (during the previous high discharge period plus the period of presence of the ETM). In the driest years, less sediment is exported to the sea, it accumulates, resulting in a higher concentration of SPM within the ETM. The authors also established that floods from the watershed play a more significant role in the sediment flushing downstream than in increasing the concentration of ETM (Jalón-Rojas et al., 2015). On the other hand, it has been suggested that when the historically accumulated pool of mobile sediment significantly exceeds the annual input from the watershed, SPM is not limited by fluvial supply and becomes more dependent on tidal energy (Schoellhamer, 2011; Burchard et al., 2018).

The Guadalquivir estuary exhibits an opposite trend, characterised by a highly turbid wet-cold season and a less turbid dry-hot season (Caballero et al., 2011; González-Ortegón and Drake, 2012; Ruiz et al., 2017). Even during the wet season, low discharges into the estuary from the Guadalquivir River are the norm, typically less than 40 m^3/seg. This is not only due to the rainfall regime in the region, but primarily due to strong water regulation practices (Díez-Minguito et al., 2012; Ruiz et al., 2017). In this context, events similar to the one described in this study are common. These events are characterised by a short-duration freshet that discharges a substantial amount of sediment into the estuary, followed by a significant reduction in river flow, which traps the SPM within the estuary, resulting in an extreme turbidity event.

Upon examining the time series data provided by Ruiz et al. (2017) in their Fig. 5, it becomes evident that after a peak in river flow, when followed by a significant and sustained reduction in discharge (e.g., in 2008–April and 2009–February), exceptionally high turbidity persists for months following the freshet. Similarly, González-Ortegón et al. (2010) also found, in the case of the Guadalquivir estuary, that persistent events of high turbidity usually start after strong and sudden freshwater discharges, following relatively long periods of very low freshwater inflow, which is a common occurrence in this region. Furthermore, the data presented in Ruiz et al. (2017) indicate that during periods of sustained high discharges (e.g., 2009–December to 2010–March, with average daily flow exceeding 1000 m^3/seg), high turbidity does not extend beyond the duration of the freshet, suggesting that the sediment is efficiently exported to the sea. This observation is consistent with the recurrent formation of a large turbidity plume seaward of the mouth of the Guadalquivir River (e.g., Fig. 3 in this study and Figure 10 in Navarro et al., 2012). This plume serves as evidence of both substantial sediment input from the watershed and significant export capacity.

However, sustained high river flows, which occur seasonally in other rainier regions (Vinh and Ouillon, 2021), are infrequent in the Guadalquivir basin. These high flows are associated with occasional periods when precipitation is abundant and persistent enough to surpass the retention capacity of the dam network within the basin (Ruiz et al., 2017). Furthermore, a crucial distinction from other European hyperturbid estuaries lies in the fact that extreme turbidity never reaches the summer months in the Guadalquivir estuary (Ruiz et al., 2017). This suggests that certain mechanisms are at work, removing SPM from the water column. Whether this removal is primarily due to the exportation of SPM to the sea, effective deposition on the estuary bed, or a combination of several mechanisms remains unclear.

Nevertheless, the limited pool of resuspendable sediment remaining during summer prevents the formation of highly turbid conditions at that season. This highlights that the development of extreme and persistent turbidity events is closely linked to the input of sediment from the watershed, and that the maximum turbidity levels are controlled by the fluvial supply: the tidal strength does not change from the wet to dry season, but the turbidity does. While tidal resuspension of particulate matter plays a significant role in generating and maintaining turbidity in the Guadalquivir estuary, leading to cyclical variability (tidally, fortnightly; Díez-Minguito et al., 2014; Ruiz et al., 2017), the overall turbidity level achieved is dependent on the previous sediment input from the watershed. Despite the moderate tidal currents in the mesotidal Guadalquivir estuary having less resuspension capacity than macrotidal and hypertidal systems, the global turbidity level reached during extreme events is comparable to, or even higher than, many of these other estuaries.

4.3. Light availability and oxygen

Other critical variables strongly affected by turbidity are light and oxygen (Ruiz et al., 2017). Light limitation has been identified as an essential characteristic of the Guadalquivir estuary (Ruiz et al., 2015, 2017). During this extreme turbidity event, light was virtually blocked at the surface throughout most of the estuary. In fact, considering that Z_{eu} finishes where 1% of the incident PAR measured on the surface reaches (Pilgrim 1987), it was found to be shallower than 10 cm upstream of the isohaline of 15 psu. As a result, primary production in the water column, as well as biogenic oxygen production through photosynthesis, were severely restricted.

The hypoxic conditions observed during this event indicate intense bacterial activity that is not compensated by biogenic oxygen production or atmospheric oxygen diffusion (Uncles et al., 1998; Ruiz et al., 2017). This process has been described as a recurrent phenomenon in the Guadalquivir estuary, particularly in its uppermost and less saline stretches (Ruiz et al., 2015, 2017). These authors argued that turbidity, rather than passive advection of less saline hypoxic water, is the primary driver of this process. This finding is supported here by the clear association between the minimum oxygen saturation and the maximum concentration of SPM, with oxygen levels increasing upstream where the salinity is equal to or lower than in the core ETM. During this event, extreme light limitation prevents the conventional eutrophication process, in which excessive *in situ* phytoplankton production is not processed by consumers and ultimately degraded by bacteria. Instead, this scenario points to the origin being the degradation of allochthonous riverine organic matter under light-limiting conditions. This mechanism is typical in the upper reaches of many turbid estuaries (Uncles et al.,

1998) and aligns with the essential mechanism proposed for these processes in the Guadalquivir estuary (Ruiz et al., 2015, 2017).

4.4. Implications for management

The available evidence highlights the critical importance of managing water discharges from the last dam to mitigate extreme turbidity processes and their subsequent environmental consequences. These consequences encompass potential impacts on essential ecosystem services, such as the estuary nursery function, filtering services, leisure use, and related industries, including fisheries, aquaculture, salt production, and tourism. To address this problem, several recommendations can be made.

First, the establishment of a permanent monitoring programme for these processes is necessary, with a particular focus on extreme events. As explained earlier, these events can be predicted based on information provided by the water management administration (Confederación Hidrográfica del Guadalquivir, www.chguadalquivir.es: CHG) through their network of sensors across the watershed (Sistema Automático de Información Hidrológica, www.chguadalquivir.es/saih). Furthermore, satellite imagery, as shown in Fig. 2, can easily identify these extreme events. Implementing such a monitoring programme would enable timely management actions to be taken during extreme events.

Second, it is crucial to incorporate the impact of water discharges into the decision-making process and dam management protocols, as recommended by previous authors (González-Ortegón et al., 2010). Considering the predicted and observed intensification of the hydrological cycle and extreme rainfall events due to global climate change (Fischer and Knutti, 2015), it becomes imperative to adopt more suitable agricultural practices in catchment areas with Mediterranean climatic regimes. For example, techniques such as the introduction of vegetal covers to promote soil retention. However, given the extensive agricultural land in the Guadalquivir River basin area, achieving this optimal mitigation approach may require a medium to long-term strategy. Meanwhile, the development of an effective water discharge protocol, taking into account factors such as the spring-neap cycle, wind, and other local climatic variables (Contreras, 2012), can be readily implemented.

Considering the scarcity of freshwater, particularly in regions facing high water stress such as the southern Iberian Peninsula (Tockner et al., 2009), and its essential role in agriculture and human consumption, a well-developed predictive model for water discharges is necessary. Hydrological models have already been developed for the Guadalquivir estuary (Siles-Ajamil et al., 2019), and the University of Málaga (J. García Lafuente, personal communication), in collaboration with the Port Authority of Seville, is currently calibrating an advanced model. This model has the potential to provide valuable information to explore alternative water discharge protocols, which should be validated and calibrated with field data.

Furthermore, the impact of freshets on plankton assemblages of the Guadalquivir estuary has already been documented in the scientific literature (Drake et al., 2007; González-Ortegón et al., 2012; González-Ortegón and Drake, 2012). Additionally, ongoing research is currently analysing the effect of discharges with varying intensities (unpublished data). The insights gained from this research will play an important role in the development of effective management strategies.

Therefore, the accumulation of robust information and expertise within multidisciplinary scientific teams has allowed the establishment of an optimal water discharge protocol for this estuary. This protocol should identify optimal periods, flows, and durations to maximise sediment export to the sea, minimise plankton washout, and prevent freshwater loss. This would result in a valuable short-to medium-term management tool, contributing significantly to the goals set forth by the EU Water Framework Directive (Chícharo et al., 2006).

5. Conclusions

The Guadalquivir estuary is one of the most turbid estuaries worldwide, particularly during recurrent events of extreme turbidity. This characteristic is remarkable given its mesotidal nature, implying a lower capacity for sediment tidal resuspension compared to many other hyperturbid estuaries. And in fact, the development of these hyperturbid events is more closely associated with the input of sediment from the highly erodible catchment area rather than tidal resuspension. Consequently, these events typically develop after short freshets followed by a sharp reduction in river flow due to strong regulation of water by the network of dams in the watershed. This process effectively traps sediment within the estuary, where it can remain accumulated for months.

The negative environmental consequences of these extreme events include a severe restriction in light availability in most of the estuary and an associated reduction in oxygen concentration, reaching hypoxic conditions in the zones with higher concentration of SPM. However, it is essential to recognise that the estuary possesses a notable capacity to get rid of SPM, and the exceptionally high concentrations observed during wet periods within hyperturbid events do not persist into the summer months. This observation presents a significant research objective for exploring potential management strategies.

Thus, directing attention towards addressing the input of sediment from the catchment area will allow short-term environmental management of this issue. The accumulation of reliable information and expertise within multidisciplinary scientific teams has enabled the development of an optimal protocol for water discharges, which is the primary recommendation derived from the evidence presented here.

Declaration of generative AI and AI-assisted technologies in the writing process

During the revision of this work, the authors used 'Writefull for Word' and 'ChatGPT' to improve English and readability. Subsequently, a professional proofreading service reviewed this draft. After using these tools and services, the authors reviewed and edited the content as needed and take full responsibility for the content of the publication.

Declaration of competing interest

The authors declare that they have no known competing interests that could have influenced the work reported in this paper.

Data availability

Data will be made available on request.

Acknowledgements

We thank Autoridad Portuaria de Sevilla for financial support and Acuario de Sevilla for logistical support. This work was partially supported by Ministerio de Universidades through two post-doctoral grants 'Margarita Salas' financed by the European Union (NextGeneration EU) (I. Donázar-Aramendía, J.M. Miró). We thank to Confederación Hidrográfica del Guadalquivir (Ministerio para la Transición Ecológica y el Reto Demográfico) and Puertos del Estado (Ministerio de Transportes, Movilidad y Agenda Urbana) for hydrological and oceanographical data support.

Appendix A. Supplementary data

Supplementary data to this article can be found online at https://doi.org/10.1016/j.ocecoaman.2023.106903.

References

Baena-Escudero, R., Rinaldi, M., García-Martínez, B., Guerrero-Amador, I.C., Nardi, L., 2019. Channel adjustments in the lower Guadalquivir River (southern Spain) over the last 250 years. Geomorphology 337, 15–30. https://doi.org/10.1016/j.geomorph.2019.03.027.

Bilotta, G.S., Brazier, R.E., 2008. Understanding the influence of suspended solids on water quality and aquatic biota. Water Res. 42, 2849–2861. https://doi.org/10.1016/j.watres.2008.03.018.

Bruton, M.N., 1985. The effects of suspensoids on fish. Hydrobiologia 125, 221–241.

Buendia, C., Herrero, A., Sabater, S., Batalla, R.J., 2016. An appraisal of the sediment yield in western Mediterranean river basins. Elsevier B.V Sci. Total Environ. 572, 538–553. https://doi.org/10.1016/j.scitotenv.2016.08.065.

Burchard, H., Schuttelaars, H.M., Ralston, D.K., 2018. Sediment trapping in estuaries. Ann. Rev. Mar. Sci 10, 371–395. https://doi.org/10.1146/annurev-marine-010816-060535.

Caballero, I., Morris, E.P., Ruiz, J., Navarro, G., 2014. Assessment of suspended solids in the Guadalquivir estuary using new DEIMOS-1 medium spatial resolution imagery. Elsevier Inc. Rem. Sens. Environ. 146, 148–158. https://doi.org/10.1016/j.rse.2013.08.047.

Caballero, I., Navarro, G., 2016. Multi-sensor analysis to study turbidity patterns in the guadalquivir estuary | Análisis multisensor para el estudio de los patrones de turbidez en el estuario del Guadalquivir, 2016 Revista de Teledeteccion 1–17. https://doi.org/10.4995/raet.2016.5717.

Caballero, I., Ruiz, J., Navarro, G., 2011. Dynamics of the turbidity plume in the Guadalquivir estuary (SW Spain): a remote sensing approach. In: OCEANS 2011 IEEE - Spain. https://doi.org/10.1109/Oceans-Spain.2011.6003489. Ieee: 1–11.

Carpintero, M., Contreras, E., Millares, A., Polo, M.J., 2013. Estimation of turbidity along the Guadalquivir estuary using Landsat TM and ETM+ images. In: Neale, C.M.U., Maltese, A. (Eds.), Proc. SPIE 8887, Remote Sensing for Agriculture, Ecosystems, and Hydrology XV, 8887:15. International Society for Optics and Photonics. https://doi.org/10.1117/12.2029183.

Chícharo, L., Chícharo, M.A., Ben-hamadou, R., 2006. Use of a hydrotechnical infrastructure (Alqueva Dam) to regulate planktonic assemblages in the Guadiana estuary: basis for sustainable water and ecosystem services management. Estuar. Coast Shelf Sci. 70, 3–18. https://doi.org/10.1016/j.ecss.2006.05.039.

Contreras, E., 2012. Influencia de los aportes fluviales en la calidad del agua del estuario del Guadalquivir. Publicaciones de la Universidad de Córdoba. Campus de Rabanales, p. 225.

Díez-Minguito, M., Baquerizo, A., Ortega-Sánchez, M., Navarro, G., Losada, M.A., 2012. Tide transformation in the Guadalquivir estuary (SW Spain) and process-based zonation. J. Geophys. Res. 117, C03019 https://doi.org/10.1029/2011JC007344.

Díez-Minguito, M., Baquerizo, A., Swart, H.E., Losada, M.A., 2014. Structure of the turbidity field in the Guadalquivir estuary: analysis of observations and a box model approach. J. Geophys. Res.: Oceans 119, 7190–7204. https://doi.org/10.1002/2014JC010210.

Donázar-Aramendía, I., Sánchez-Moyano, J.E., García-Asencio, I., Miró, J.M., Megina, C., García-Gómez, J.C., 2018. Maintenance dredging impacts on a highly stressed estuary (Guadalquivir estuary): a BACI approach through oligohaline and polyhaline habitats. Mar. Environ. Res. 140 https://doi.org/10.1016/j.marenvres.2018.07.012. Elsevier: 455–467.

Donázar-Aramendía, I., Sánchez-Moyano, J.E., García-Asencio, I., Miró, J.M., Megina, C., García-Gómez, J.C., 2019. Human pressures on two estuaries of the Iberian Peninsula are reflected in food web structure. Sci. Rep. 9, 1–10. https://doi.org/10.1038/s41598-019-47793-2.

Drake, P., Borlán, A., González-Ortegón, E., Baldó, F., Vilas, C., Fernández-Delgado, C., 2007. Spatio-temporal distribution of early life stages of the European anchovy Engraulis encrasicolus L. within a European temperate estuary with regulated freshwater inflow: effects of environmental variables. J. Fish. Biol. 70, 1689–1709. https://doi.org/10.1111/j.1095-8649.2007.01433.x.

Fernández-Nóvoa, D., deCastro, M., Des, M., Costoya, X., Mendes, R., Gómez-Gesteira, M., 2017. Characterization of Iberian turbid plumes by means of synoptic patterns obtained through MODIS imagery. J. Sea Res. 126 https://doi.org/10.1016/j.seares.2017.06.013. Elsevier: 12–25.

Fischer, E.M., Knutti, R., 2015. Anthropogenic contribution to global occurrence of heavy-precipitation and high-temperature extremes. Nat. Clim. Change 5, 560–564. https://doi.org/10.1038/nclimate2617.

García-Martínez, B., Rinaldi, M., 2022. Changes in meander geometry over the last 250 years along the lower Guadalquivir River (southern Spain) in response to hydrological and human factors. Geomorphology 410. https://doi.org/10.1016/j.geomorph.2022.108284.

González-Ortegón, E., Drake, P., 2012. Effects of freshwater inputs on the lower trophic levels of a temperate estuary: physical, physiological or trophic forcing? Aquat. Sci. 74, 455–469. https://doi.org/10.1007/s00027-011-0240-5.

González-Ortegón, E., Subida, M.D., Arias, A.M., Baldó, F., Cuesta, J.A., Fernández-Delgado, C., Vilas, C., Drake, P., 2012. Nekton response to freshwater inputs in a temperate European estuary with regulated riverine inflow. Elsevier B.V Sci. Total Environ. 440. https://doi.org/10.1016/j.scitotenv.2012.06.061, 261–71.

González-Ortegón, E., Subida, M.D., Cuesta, J.A., Arias, A.M., Fernández-Delgado, C., Drake, P., 2010. The impact of extreme turbidity events on the nursery function of a temperate European estuary with regulated freshwater inflow. Estuar. Coast Shelf Sci. 87, 311–324. https://doi.org/10.1016/j.ecss.2010.01.013.

Grasso, F., Verney, R., le Hir, P., Thouvenin, B., Schulz, E., Kervella, Y., Khojasteh, I., et al., 2018. Suspended sediment dynamics in the macrotidal seine estuary (France): 1. Numerical modeling of turbidity maximum dynamics. J. Geophys. Res.: Oceans 123, 558–577. https://doi.org/10.1002/2017JC013185.

Hecht, T., van der Lingen, C.D., 1992. Turbidity-induced changes in feeding strategies of fish in estuaries. S. Afr. J. Zool. 27, 95–107. https://doi.org/10.1080/02541858.1992.11448269.

Jalón-Rojas, I., Schmidt, S., Sottolichio, A., 2015. Turbidity in the fluvial Gironde Estuary (southwest France) based on 10-year continuous monitoring: sensitivity to hydrological conditions. Hydrol. Earth Syst. Sci. 19, 2805–2819. https://doi.org/10.5194/hess-19-2805-2015.

Jalón-Rojas, I., Schmidt, S., Sottolichio, A., 2017. Comparison of environmental forcings affecting suspended sediments variability in two macrotidal, highly-turbid estuaries. Academic Press Estuar. Coast Shelf Sci. 198. https://doi.org/10.1016/j.ecss.2017.02.017, 529–541.

Jalón-Rojas, I., Schmidt, S., Sottolichio, A., Bertier, C., 2016. Tracking the turbidity maximum zone in the Loire Estuary (France) based on a long-term, high-resolution and high-frequency monitoring network. In: Continental Shelf Research, vol. 117. https://doi.org/10.1016/j.csr.2016.01.017. Elsevier: 1–11.

Jay, D.A., Orton, P.M., Chisholm, T., Wilson, D.J., Fain, A.M.V., 2007. Particle trapping in stratified estuaries: application to observations. Estuar. Coast 30, 1106–1125. https://doi.org/10.1007/BF02841400.

Kirk, J.T.O., 1994. Light & Photosynthesis in Aquatic Ecosystems. Cambridge University Press, p. 509.

Llope, M., 2017. The ecosystem approach in the Gulf of Cadiz. A perspective from the southernmost European Atlantic regional sea. ICES (Int. Counc. Explor. Sea) J. Mar. Sci. 74, 382–390. https://doi.org/10.1093/icesjms/fsw165.

Milliman, J.D., Farnsworth, K.L., 2011. River discharge to the coastal ocean. In: A Global Synthesis. Cambridge University Press. https://doi.org/10.1017/CBO9780511781247.

Miró, J.M., Megina, C., Donázar-Aramendía, I., García-Gómez, J.C., 2022. Effects of maintenance dredging on the macrofauna of the water column in a turbid estuary. Sci. Total Environ. 806 https://doi.org/10.1016/j.scitotenv.2021.151304.

Miró, J.M., Megina, C., Donázar-aramendía, I., Reyes-martínez, M.J., 2020. Environmental factors affecting the nursery function for fish in the main estuaries of the Gulf of Cadiz (south-west Iberian Peninsula). Elsevier B.V. Sci. Total Environ. 737, 139614 https://doi.org/10.1016/j.scitotenv.2020.139614.

Mitchell, S.B., 2013. Turbidity maxima in four macrotidal estuaries. Elsevier Ltd Ocean Coast Manag. 79, 62–69. https://doi.org/10.1016/j.ocecoaman.2012.05.030.

Mitchell, S.B., Uncles, R.J., 2013. Estuarine sediments in macrotidal estuaries: future research requirements and management challenges. Ocean Coast Manag. 79, 97–100. https://doi.org/10.1016/j.ocecoaman.2012.05.007. Elsevier.

Modéran, J., Bouvais, P., David, V., le Noc, S., Simon-Bouhet, B., Niquil, N., Miramand, P., Fichet, D., 2010. Zooplankton community structure in a highly turbid environment (Charente estuary, France): spatio-temporal patterns and environmental control. Elsevier Ltd Estuar. Coast Shelf Sci. 88, 219–232. https://doi.org/10.1016/j.ecss.2010.04.002.

Navarro, G., Gutiérrez, F.J., Díez-Minguito, M., Losada, M.A., Ruiz, J., 2011. Temporal and spatial variability in the Guadalquivir estuary: a challenge for real-time telemetry. Ocean Dynam. 61, 753–765. https://doi.org/10.1007/s10236-011-0379-6.

Navarro, G., Huertas, I.E., Costas, E., Flecha, S., Díez-Minguito, M., Caballero, I., López-Rodas, V., Prieto, L., Ruiz, J., 2012. Use of a real-time remote monitoring network (RTRM) to characterize the Guadalquivir estuary (Spain). Sensors 12, 1398–1421. https://doi.org/10.3390/s120201398.

Pilgrim, D.A., 1987. Measurement and estimation of the extinction coefficient in turbid estuarine waters. Continent. Shelf Res. 7, 1425–1428. https://doi.org/10.1016/0278-4343(87)90049-5.

Piton, V., Ouillon, S., Vinh, V.D., Many, G., Herrmann, M., Marsaleix, P., 2020. Seasonal and tidal variability of the hydrology and suspended particulate matter in the Van Uc estuary, Red River, Vietnam. Elsevier J. Mar. Syst. 211, 103403. https://doi.org/10.1016/j.jmarsys.2020.103403.

R Core Team, 2022. R: A Language and Environment for Statistical Computing. R Foundation for Statistical Computing, Vienna, Austria. URL. https://www.R-project.org/.

Ruiz, J., Macías, D., Navarro, G., 2017. Natural forcings on a transformed territory overshoot thresholds of primary productivity in the Guadalquivir estuary. Elsevier Ltd Continent. Shelf Res. 148, 199–207. https://doi.org/10.1016/j.csr.2017.09.002.

Ruiz, J., Polo, M.J., Díez-Minguito, M., Navarro, G., Morris, E.P., Huertas, E., Caballero, I., Contreras, E., Losada, M.A., 2015. The guadalquivir estuary: a hot spot for environmental and human conflicts. In: Environmental Management and Governance. Coastal Research Library, vol. 8, pp. 199–232. https://doi.org/10.1007/978-3-319-06305-8.

Sabater, S., Feio, M.J., Graça, M.A.S., Muñoz, I., Romaní, A.M., 2009. The iberian rivers. In: Tockner, K., Uehlinger, U., Robinson, C.T. (Eds.), Rivers of Europe, vols. 113–149. Academic Press, Elsevier Ltd, New York, NY. https://doi.org/10.1016/B978-0-12-369449-2.00004-7.

Schlitzer, Reiner, 2021. Ocean Data View. http://odv.awi.de.

Schmidt, S., Diallo, I.I., Derriennic, H., Fallou, H., Lepage, M., 2019. Exploring the susceptibility of turbid estuaries to hypoxia as a prerequisite to designing a pertinent monitoring strategy of dissolved oxygen. Front. Mar. Sci. 6, 1–8. https://doi.org/10.3389/fmars.2019.00352.

Schoellhamer, D.H., 2011. Sudden clearing of estuarine waters upon crossing the threshold from transport to supply regulation of sediment transport as an erodible sediment pool is depleted: San Francisco bay, 1999. Estuar. Coast 34, 885–899. https://doi.org/10.1007/s12237-011-9382-x.

Siles-Ajamil, R., Díez-Minguito, M., Losada, M., 2019. Tide propagation and salinity distribution response to changes in water depth and channel network in the Guadalquivir River Estuary: an exploratory model approach. Ocean Coast Manag. 174 https://doi.org/10.1016/j.ocecoaman.2019.03.015. Elsevier: 92–107.

Tockner, K., Uehlinger, U., Robinson, C.T., Tonolla, D., Siber, R., Peter, F.D., 2009. Introduction to European rivers. In: Tockner, K., Uehlinger, U., Robinson, C.T. (Eds.), Rivers of Europe, vols. 1–21. Academic Press, Elsevier Ltd, New York, NY. https://doi.org/10.1016/B978-0-12-369449-2.00001-1.

Toublanc, F., Brenon, I., Coulombier, T., 2016. Formation and structure of the turbidity maximum in the macrotidal Charente estuary (France): influence of fluvial and tidal forcing. Elsevier Ltd Estuar. Coast Shelf Sci. 169, 1–14. https://doi.org/10.1016/j.ecss.2015.11.019.

Uncles, R.J., Joint, I., Stephens, J.A., 1998. Transport and retention of suspended particulate matter and bacteria in the Humber-Ouse Estuary, United Kingdom, and their relationship to hypoxia and anoxia. Estuaries 21, 597–612. https://doi.org/10.2307/1353298.

Uncles, R.J., Stephens, J.A., Harris, C., 2013. Estimating estuarine turbidity: an application to estuaries of the Isle of Man and northeast Irish Sea. Elsevier Ltd Ocean Coast Manag. 79, 42–51. https://doi.org/10.1016/j.ocecoaman.2012.05.013.

Uncles, R.J., Stephens, J.A., Law, D.J., 2006. Turbidity maximum in the macrotidal, highly turbid Humber Estuary, UK: flocs, fluid mud, stationary suspensions and tidal bores. Estuar. Coast Shelf Sci. 67, 30–52. https://doi.org/10.1016/j.ecss.2005.10.013.

Uncles, R.J., Stephens, J.A., Smith, R.E., 2002. The dependence of estuarine turbidity on tidal intrusion length, tidal range and residence time. Continent. Shelf Res. 22, 1835–1856. https://doi.org/10.1016/S0278-4343(02)00041-9.

Utne-Palm, A.C., 2002. Visual feeding of fish in a turbid environment: physical and behavioural aspects. Mar. Freshw. Behav. Physiol. 35, 111–128. https://doi.org/10.1080/10236240290025644.

Vinh, V.D., Ouillon, S., 2021. The double structure of the estuarine turbidity maximum in the cam-nam Trieu mesotidal tropical estuary, Vietnam. Elsevier B.V. Mar. Geol. 442, 106670 https://doi.org/10.1016/j.margeo.2021.106670.

Vörösmarty, C.J., Meybeck, M., Fekete, B., Sharma, K., Green, P., Syvitski, J.P.M., 2003. Anthropogenic sediment retention: major global impact from registered river impoundments. Global Planet. Change 39, 169–190. https://doi.org/10.1016/S0921-8181(03)00023-7.

Wang, Z.B., Winterwerp, J.C., He, Q., 2014. Interaction between suspended sediment and tidal amplification in the Guadalquivir Estuary. Ocean Dynam. 64, 1487–1498. https://doi.org/10.1007/s10236-014-0758-x.

Winterwerp, J.C., Wang, Z.B., van Braeckel, A., van Holland, G., Kösters, F., 2013. Man-induced regime shifts in small estuaries—II: a comparison of rivers. Ocean Dynam. 63, 1293–1306. https://doi.org/10.1007/s10236-013-0663-8.

Wolanski, E., 2004. Ecohydrology as a new tool for sustainable management of estuaries and coastal waters. Wetl. Ecol. Manag. 12, 235–276.

Wood, S.N., 2017. Generalized Additive Models: an Introduction with R, second ed. Chapman and Hall/CRC.

Zorrilla-Miras, P., Palomo, I., Gómez-Baggethun, E., Martín-López, B., Lomas, P.L., Montes, C., 2014. Effects of land-use change on wetland ecosystem services: a case study in the Doñana marshes (SW Spain). Elsevier B.V. Landsc. Urban Plann. 122, 160–174. https://doi.org/10.1016/j.landurbplan.2013.09.013.